HHS Public Access

Author manuscript

Nat Med. Author manuscript; available in PMC 2013 March 01.

Published in final edited form as:

Nat Med. 2012 September ; 18(9): 1413–1417. doi:10.1038/nm.2886.

Decreased Expression of Synapse-Related Genes and Loss of Synapses in Major Depressive Disorder

H.J. Kang[1], **B. Voleti**[1], **T. Hajszan**[3,4], **G. Rajkowska**[5], **C. Stockmeier**[5], **P. Licznerski**[1], **A. Lepack**[1], **M.S. Majik**[6], **L.S. Jeong**[6], **M. Banasr**[1], **H. Son**[7], and **R.S. Duman**[1,2]

[1]Depts. of Psychiatry, New Haven, CT, USA

[2]Depts. of Neurobiology, and New Haven, CT, USA

[3]Depts. of OBGYN Yale University, New Haven, CT, USA

[4]Dept. of Biophysics, Biological Research Center, Hungarian Academy of Sciences, Szeged, Hungary

[5]Dept. Psychiatry & Human Behavior, University of Mississippi Medical Center, Jackson, MS

[6]Dept. of Bioinspired Science, and Laboratory of Medicinal Chemistry, College of Pharmacy, Ewha Womans University, Seoul, Korea

[7]Dept. of Biochemistry and Molecular Biology, Hanyang University College of Medicine, Seoul, Korea

Abstract

Previous imaging and postmortem studies have reported a reduction in brain volume and a decrease in the size and density of neurons in the dorsolateral prefrontal cortex (dlPFC, area 9) of subjects with major depressive disorder (MDD).[1,2] These findings suggest that synapse number and function are decreased in dlPFC of depressed patients. However, there has been no direct evidence for synapse loss in MDD and the gene expression alterations underlying these effects have not been identified. Here we use microarray gene profiling and electron microscopic

Correspondence:, Ronald S. Duman, Ph.D., Professor of Psychiatry and Pharmacology, Director, Abraham Ribicoff Research Facilities, Laboratory of Molecular Psychiatry, Yale University School of Medicine, 34 Park Street, room 308, New Haven, CT 06508, Phone: (203) 974-7726, Fax: (203) 974-7724, ronald.duman@yale.edu.

Author Contributions

H.J.K was involved in planning and conducting all aspects of the research, including analysis of microarray data, confirmation of results, molecular and cellular experiments, and construction of the viral vectors; H.J.K. also prepared the first draft of the manuscript. B.V. designed viral vectors, conducted the behavioral studies and was involved in the analysis and interpretation of rodent behavioral studies, C.A.S. and G.R. were responsible for generation of relevant human subjects' information tables and methodology, and for preparation of human tissue and microdissections. T.H. conducted electron microscopy analysis of synapse number in postmortem tissue. M.B. with the technical help of A.L. carried out the rat CUS studies and prepared tissues for in situ hybridization analysis, animal surgeries and supervised behavioral studies. P.L. was involved in the viral vector preparations and H.S. was involved in viral vector experiments, including surgical infusions, behavioral studies, and immunohistochemistry. M.S.M and L.S.J synthesized the GATA1 specific inhibitor, K-7174. R.S.D. was responsible for overseeing the study, including all aspects of study design, data analysis, interpretation of results and preparation of the manuscript and figures. All authors discussed the results presented in the manuscript.

Competing Financial Interests

The authors declare no financial interests.

stereology to reveal decreased expression of synaptic function-related genes in dlPFC of MDD subjects and a corresponding reduction in the number of synapses. We also identify a transcriptional repressor that is increased in MDD, and that when expressed in PFC neurons is sufficient to decrease expression of synapse-related genes, cause loss of spines and dendrites, and produce depressive behavior in rodent models of depression.

Keywords

postmortem; stress; prefrontal cortex; microarray; transcription factor; repressor

Major depressive disorder (MDD) affects approximately 17 percent of the population, and is predicted to be the number two cause of illness worldwide by the year 2020[3]. The symptoms include cognitive impairment and loss of memory, implicating synaptic dysfunction in the pathophysiology of MDD[4–6]. This possibility is supported by studies demonstrating a reduction of dendritic spine number and function of neurons in PFC in animal models of depression[7,8]. Postmortem studies also report morphometric changes in PFC of MDD subjects, including a reduction in neuronal body size[1,9]. This is also consistent with brain imaging studies reporting a reduction in the volume of PFC subregions in MDD subjects[2,10]. Together, these studies suggest a loss of spine number and dendritic arbor although there is no direct evidence demonstrating this type of neuronal atrophy in the brains of MDD subjects.

To gain insight into the mechanisms that underlie neuronal atrophy and reduced volume of PFC, we have re-analyzed the data from a prior microarray gene expression study that we conducted of the dlPFC (Brodmann area 9) of MDD subjects and matched controls[11]. We classified the microarray data with a 5% FDR[11]and found that about 30% of the down-regulated genes in the MDD group could be related to some aspect of synaptic function. A more extended range (20% cutoff) identified an additional subset of down-regulated synaptic function-related genes in dlPFC of MDD brains (Table 1). The synaptic categories include regulation of synaptic vesicles [calmodulin 2, synapsins I and III, Rab3A, amphiphysin, and synaptogyrin 3][12–16]regulation of synaptic strength [neurogranin][17]dendritic spine formation [Rab4B][18], and axonal outgrowth and regeneration [tubulins][19]. It is notable that other genome-wide expression studies of MDD have reported gene alterations of similar functional categories, including cytoarchitecture, vesicular transport, and synaptic transmission, of some of the same synapse-related genes[20–23]or isoforms of the genes identified here (e.g., subtypes of amphiphysin, synaptogyrin, synapsin, and the Ras superfamily[22–24].

PCR analysis demonstrated significant decreases for 5 of the 10 genes, and trends for all but one (amphiphysin) of the remaining genes in the dlPFC of MDD subjects (Table 1). In situ hybridization analysis of the five confirmed genes demonstrates enriched expression in gray matter of dlPFC with a laminar distribution in the middle (synapsin I) or middle and deep layers (calmodulin 2, Rab3A, Rab4B and β-tubulin 4) of dlPFC. Quantitative analysis confirms that levels of these five genes are significantly decreased in MDD subjects compared to controls (Fig. 1a–e). Studies in rodents demonstrate that chronic unpredictable

stress (CUS), considered one of the most valid rodent models of depression, decreases the expression of synapsin I, calmodulin 2, Rab3A, and Rab4B, but not beta-tubulin 4, in the PFC (Supplementary Fig. 1), suggesting that the decreased levels of these synapse-related genes in MDD result from chronic stress exposure that could contribute to depressive behaviors.

Decreased expression of synapse-related genes shown here, and a previous report of reduced neuronal cell body size in the dlPFC of MDD subjects[1], suggest a reduction in synaptic density, although there is no direct evidence to support this possibility. Examination of dendritic morphology by microtubule-associated protein 2 (MAP2) immunohistochemistry revealed decreased staining of dendritic processes in dlPFC layers III through V of MDD subjects relative to controls, which was confirmed by MAP2 immunoblotting of dlPFC micro-punches (Fig. 1f,g). Using electron microscopic stereological analysis, a marked decrease in spine synapse number was observed in MDD subjects compared to controls (Fig. 1h). Co-factor analysis revealed no significant effects of medication status, age of first episode (<40 vs. ≥40 years old), or suicide on synapse number (Supplementary Figs. 2, 3, 5).

Examination of the transcription factor binding motifs in the promoter regions of the decreased synapse-related genes identified 3,266 upstream regulatory elements for 218 transcription factors (TRANSFAC scoring matrix, Supplementary Table 1). Twelve transcription factor-binding sites are localized to the upstream regulatory domain of all of the MDD and CUS-altered synapse-related genes (Fig. 2a). The rat homologues of these synapse-related genes include eight of the twelve transcription factor regulatory elements (Fig. 2a and Supplementary Table 2). Analysis of the microarray data revealed that one of these transcription factors *GATA1* is significantly increased in MDD patients (Fig. 2b). Other transcriptions factors were either not significantly changed in MDD (*GKLF* and *KID3*1.0- and 1.1-fold, respectively) or were not included in the microarray gene set. Levels of the related *GATA-2*, *3*, and *4* isoforms were not significantly altered in MDD compared to controls. Co-factor analysis revealed no effect of medication status on *GATA1* expression, and no significant differences between all MDD subjects and groups categorized by age of first episode, number of episodes, and suicide, although the number of subjects per subgroup was small (Supplementary Figs. 2–5). Studies in the CUS rodent model of depression demonstrate increased *Gata1* expression in the PFC, which was completely reversed by chronic administration of fluoxetine (Fig. 2c). The ability of antidepressant treatment to normalize *Gata1* expression in rodents but not in MDD could be due to the small number of the medicated and un-medicated subgroups, as well as treatment resistance and heterogeneity of the subjects. The binding activity of Gata1 to the promoter of the synapse related genes was confirmed by chromatin immunoprecipitation (ChIP) with a Gata1 antibody followed by PCR for the Gata1 binding region of each gene (Fig. 2d). For most of the genes, Gata1 antibody ChIP resulted in an enrichment of the promoter compared to mock, control ChIP.

The possibility that elevated GATA1 underlies decreased expression of the synapse-related genes and the atrophy of dendritic processes was examined in primary neuronal cultures. Initial studies focused on Rab4B because this class of small GTP-binding protein is required for endosomal recycling that is critical for maintenance of spine size[18] and because *RAB4B*

showed the greatest reduction (Table 1). Expression of a GFP-tagged rAAV-GATA1 vector in cultured cortical neurons (Fig. 3a,b) significantly decreased the expression of *Rab4b* (Fig. 3c). Expression of a cofactor target gene, FOG1, that is positively regulated by GATA1[25,26], was significantly increased by viral expression of GATA1 (not shown). To analyze dendrite morphology, neurons were fixed and labeled with anti-GFP (Fig. 3d,e), as well as anti-MAP2 antibodies (Fig. 3f). Viral expression of GATA1 decreased the complexity of the dendritic arbor (Fig. 3d), the number of spines (Fig. 3e), and the intensity of MAP2 staining (Fig. 3f), which was confirmed by western blot analysis (Fig. 3g). Sholl analysis demonstrated that viral expression of GATA1 significantly decreased the number of dendrite intersections, indicating decreased complexity (Fig. 3h).

Next the effects of GATA1 expression on behavior in rodent models of depression were examined. Control or GATA1 viral vectors were infused into the PFC (Fig. 4a), and the expression and location were confirmed by GFP expression (Fig. 4b). Infusion of rAAV-GATA1 produced depressive-like behaviors in two established rodent models. In the forced swim test, rAAV-GATA1 increased the time spent immobile, a measure of behavioral despair that is reversed by antidepressant treatment (Fig. 4c). In the learned helplessness model, exposing animals to inescapable stress causes escape deficits that are reversed by antidepressant treatment. Infusions of rAAV-GATA1 increased the number of escape failures during the initial block of active avoidance testing, similar to the effects of inescapable stress exposure (Fig. 4d). During the second block of active avoidance testing, there was no significant effect (Fig. 4d), indicating that GATA1 delays responding, but does not produce a sustained effect in this model. Infusion of rAAV-GATA1 did not influence locomotor activity (not shown), indicating that there was no generalized effect on ambulation. Further studies showed that the effects of rAAV-GATA1 in the forced swim test were not reversed by the antidepressant imipramine as expected, since drug treatment would not influence viral expression of GATA1 (Supplementary Fig. 6).

The influence of GATA1 on depressive behavior caused by chronic stress was examined with a viral knock down strategy, using a small hairpin RNA (shRNA) targeted to GATA1 (rAAV-GATA1^{shRNA}) (Fig. 4e). The ability of rAAV-GATA1^{shRNA} to effectively decrease *Gata1* mRNA was confirmed in cultured cells and rat PFC (Supplementary Fig. 7). The rAAV-GATA1^{shRNA} or scrambled control (rAAV-Scr^{shRNA}) was infused into the PFC (Fig. 4f) of rats that were then subjected to the CUS paradigm shown to increase *Gata1* mRNA (Fig. 2c). This paradigm results in anhedonia, a core symptom of depression that can be measured by preference for a sweetened solution[27]. CUS exposure significantly decreased sucrose preference in control rats infused with rAAV-Scr^{shRNA} and this effect was completely blocked by infusion of rAAV-GATA1^{shRNA}. There was no effect of rAAV-GATA1^{shRNA} in non-stressed rats indicating that basal levels of GATA1 are low and not sufficient to suppress basal rates of sucrose preference.

Using three complimentary approaches we have identified and confirmed a subset of synapse-related genes that are repressed in dlPFC of MDD subjects. At the presynaptic level, synapsin I, Rab3A and calmodulin 2 regulate the size, number, and targeting of synaptic vesicles, and β-tubulins are involved in axonal outgrowth and regeneration[19, 28–31]. Postsynaptically, Rab4B regulates endosomal recycling that is required for spine

maintenance and neurotransmitter receptor recycling[18,32]. Consistent with the role of these genes in synaptic function and structure, our results also demonstrate a reduction in synapse numbers in dlPFC. Together these findings demonstrate molecular and cellular alterations that could underlie the reduction in neuronal cell body size and volume of PFC in MDD patients[1,10]. Decreased expression of these genes in response to chronic stress exposure also suggests an etiological relationship to MDD, which is often associated with severe life stress and trauma[33,34].

GATA1 was also identified as a transcriptional repressor that is increased in MDD and has binding elements in the promoter regions of the synapse related genes. GATA1 is a member of a zinc finger family of transcription factors that are evolutionarily conserved and play important roles in embryonic development[35]. Although originally characterized in hematopoietic and cardiac tissues, GATA transcription factors are also expressed in endocrine tissue and brain, and are reported to regulate neuronal differentiation during development[35–38]. Although GATA1 levels are low in controls, expression is increased in MDD and in response to chronic stress. Over expression of *Gata1* was sufficient to cause dendrite atrophy and decreased synaptic protein expression in cultured cortical neurons. Moreover, expression of *Gata1* in PFC was sufficient to produce depressive behaviors, while knock down of *Gata1* completely blocked depressive, anhedonic behavior caused by CUS exposure. Together, these studies demonstrate that expression of *Gata1* in the PFC is sufficient and necessary for the development of depressive behaviors in multiple animal paradigms. Further evidence for a role of GATA1 is provided by a recent report of a polymorphism in the GATA1 binding site of the promoter for interleukin 6, an inflammatory cytokine dysregulated in depression[39].

Together the results describe molecular and cellular mechanisms that are sufficient to cause a reduction in synapse numbers and dendritic complexity and could contribute to neuronal atrophy and decreased cortical volume reported in MDD patients. The results suggest that approaches that block or reverse neuronal atrophy in the PFC could be effective antidepressant treatments. This possibility is supported by recent studies demonstrating that the rapid antidepressant actions of NMDA receptor blockade are associated with increased spine number and function, and increased synaptogenesis in the PFC[40].

Online Methods

Human Subjects and Microarray Analysis

The description of postmortem tissue collection, subjects, and microarray analysis are exactly as described in our previous study[11].

Quantitative Real Time PCR

An aliquot of the total RNA that was previously extracted from prefrontal cortex punches was used for secondary validation using real time PCR. Five hundred ng of total RNA was used for cDNA synthesis using oligo dT primers and SuperScript II reverse transcriptase (Invitrogen), and subsequently diluted with nuclease-free water to 10 ng ul^{-1} cDNA. Gene-specific high-melt temperature primers for genes of interest were designed using Primer 3

software (http://frodo.wi.mit.edu/cgi-bin/primer3/primer3_www.cgi; Whitehead Institute for Biomedical Research) and expressed sequence information obtained from GenBank (NCBI). PCR reactions were conducted on an ABI 7900 Sequence Detection System (Applied Biosystems) using a hotstart SYBR-green based method (Quantitect, QIAGEN) followed by melt curve analysis to verify specificity of product. The C_T value (cycle number at threshold) was used for calculations of relative amount of mRNA molecules. The C_T value of each target genes was normalized by subtraction of the C_T value from multiple housekeeping genes. This value is the ΔC_T. The difference in ΔC_T between Control and MDD represents the $\Delta\Delta C_T$, and the relative quantitative change was showed as $2^{-\Delta\Delta C_T}$. All of the genes of interest were normalized to the housekeeping gene, cyclophilin.

Electronic Microscopic Stereology

The number of spine synapses in dlPFC of postmortem brains was counted as previously described[41,42]. Briefly, postmortem samples were immersed overnight in a mixture of 2% glutaraldehyde + 4% paraformaldehyde dissolved in phosphate buffer. Vibratome sections of 100 μm were cut throughout the tissue blocks and embedded in Durcupan (Electron Microscopy Sciences, Fort Washington, PA). Using the embedded sections, at least ten sampling areas were randomly selected from each brain, and ultrathin sections (~70 nm) from each sampling area were prepared with a Reichert Ultracut E ultrotome. Digitized electron micrographs of each sampling area were taken in a Tecnai 12 transmission electron microscope (FEI company, Hillsboro, OR). Synapses were counted using the dissector technique. Synapse numbers for each brain were obtained by averaging data from at least ten dissectors.

In situ hybridization

Sections of human brain were cut at 14 μm from blocked dlPFC. Rat brains were also sectioned at 14 μm, after animals were euthanized and brains stored at −80 °C. Brains were mounted onto ‘probe-on plus’ glass slides (Fisher Scientific). To prepare complimentary RNA probe (cRNA) for in situ hybridization histochemistry, the fragments of cDNA were amplified by PCR using T7 promoter attached primer and PCR products were used to generate ^{35}S-radiolabeled riboprobes using T7 RNA polymerase in vitro transcription (Ambion, T7-MEGAshortscript). After fixation and acetylation, human or rat sections were hybridized with ^{35}S-CTP incorporated RNA probes at 60 °C for 16 hr in the hybridization solution. Sections were then washed at 60 °C, dehydrated with graded alcohols, air-dried and exposed to film.

Stress and antidepressant model

For chronic unpredictable stress, rats were subjected to chronic unpredictable stress (CUS) for 35 days as previously described[40]; fluoxetine was administrated from day 15–35 (twice a day, 15mg kg^{-1} per treatment). Control rats were handled every other day for the first 15 days or then daily for vehicle (saline) administration and brains were harvested for in situ hybridization analysis 4 hr after the last vehicle or drug treatment. For stress study with rAAV-GATA1^{shRNA}rats were subjected to 3 weeks of chronic unpredictable stress after the viral infusion.

Transcription factor binding motif search

The scoring matrix of TRANSFAC (http://www.biobase-international.com) was used for the binding motif search in promoter regions (1 kb of the 5'-flanking sequence and 200 bp on downstream from transcription start site) of our candidate genes. The over-represented TFBSs were determined in the set of promoters with the parameter of exact matches of core sequences (Core Score = 1) at 0.95 matrix similarity cut-off (Matrix Score ≥ 0.95) in the vertebrate matrix.

Chromatin Immunoprecipitation

Cultured primary cortical neurons (DIV 7) were incubated in 1% formaldehyde for 10 min at RT for cross-linking of DNA and DNA binding proteins. Crosslinked neurons were lysed in SDS lysis buffer (1% SDS, 10 mM EDTA, 50 mM Tris-HCl, pH 8.1) including protease inhibitors and phosphatase inhibitors. Chromatin was sheared by sonication and separated by centrifugation for 10 min at 13000 rpm. The supernatant was collected and immunoprecipitated with dynabead (Dynal, 112-01D) conjugated 1 ug of anti-GATA1 (Santa Cruz, sc-265) or normal horse serum overnight at 4 °C. After reverse cross-linking, DNA was eluted using Qiagen minelute purification kit and quantified by real time PCR.

Primary cortical neuron culture

Embryonic brains were prepared from fetal SD rat at 18 d gestation and mechanically triturated as described previously[43]. Dissociated cells were plated on 12 well plates ($0.5x10^5$ cells per well) in plating medium consisting of Neurobasal media supplemented with 10% fetal bovine serum, 2 mM L-glutamine, 1 mM sodium pyruvate, 1 mM HEPES, 2% pen-strep and 2% B27 supplement. Proliferation of non-neuronal cells was halted by replacing with plating medium lacking fetal serum in the next day (DIV 1). Cultures were then fed once a week with plating medium lacking fetal serum and maintained at 37 °C in a humidified 5% CO_2 atmosphere.

Generation of rAAV vectors

To generate rAAV-GATA1-GFP, mouse GATA1 cDNA (1801 bp) was subcloned in the mammalian expression vector (pXM-GATA1) and inserted into the pAAV-EGFP-pA (5403 bp) vector by enzyme restriction and ligation. Hairpin RNA was designed to specifically target GATA1 mRNA. A 24-bp oligonucleotide sequence within the coding region of the GATA1 gene was identified. Hairpins were designed such that the antisense strand came before the sense strand during transcription. Two sets of oligonucleotides were synthesized (Integrated DNA Technologies, Coralville, Iowa) for cloning: GATA1shRNA top: 5'-TTTGAAGATGCTGTATCCAAACTCTCACTTCCTGTCATGAGAGTTTGGATACAGCATCTTATTTTT-3'; bottom: 5'-CTAGAAAAATAAGATGCTGTATCCAAACTCTCATGACAGGAAGTGAGAGTTTGGATACAGCATCTTC-3'; The oligonucleotides had Sap1 and Xba1 overhangs to allow for ligation into mU6pro region of the modified pAAV-MCS vector, pAAV-shRNA. The pAAV-shRNA plasmid was designed to coexpress small hairpin RNA (shRNA) and enhanced green fluorescent protein under the control of an independent RNA polymerase II promoter for enhanced green fluorescent protein and U6 promoter for shRNA. All final

clones were verified for sequencing. For virus preparation, HEK293 cells were co-transfected with pAAV-GATA1-EGFP or pAAV-EGFP or pAAV-ScrshRNA or pAAV-GATA1shRNA, pAAV-RC and pHelper using calcium phosphate precipitate method. After 72 hours, vectors were purified from cell lysates by iodixanol gradient centrifugation followed by column concentration. Behavioral experiments using rAAV-GATA1shRNAwere performed after ensuring efficient knockdown of GATA1 mRNA in human embryonic kidney cells (HEK293). For in vitro validation, plasmids expressing scrambled shRNA (pScrshRNA) and GATA1shRNA (pGATA1shRNA) were transfected intor HEK cells using lipofectamine (Invitrogen) following manufacturer's instructions. 24 hrs after the transfection, RNA was purified using RNaqueous kit (Ambion) and cDNA was synthesized for qPCR. For in vivo validation, animals were perfused and medial PFC was microdissected after behavioral testing. Total RNA was extracted from the PFC using RNAeasy FFPE kit (Qiagen) and quantitative RT-PCR was performed as described above.

Western blot

Cultured neurons were lysed in RIPA buffer. Protein levels were measured using BCA Protein Assay Kit. Proteins were separated by SDS-PAGE and transferred to the nitrocellulose membranes. After blocking with 10% skim milk, the blots were incubated with primary antibodies overnight at 4 °C followed by horseradish peroxidase-conjugated secondary antibodies for 1 hr at RT. Blots were visualized by enhanced chemiluminescence and exposed on films.

Immunohistochemistry

Sections were fixed in 4% paraformaldehyde-PBS for 10 min and followed by 0.6% hydrogen peroxide treatment for 5 min. Sections were incubated in a blocking solution (2.5% BSA in PBS) for 30 min, reacted with rabbit polyclonal anti-GFP (abcam, 1:500) or mouse monoclonal antibody recognizing MAP2 (Sigma, 1:200) in PBS (0.25% Triton X, 1% BSA) and then reacted with secondary antibody for 1 hr at RT.

Sholl analysis

Dendritic branching was investigated by Sholl analysis[44]. A transparent grid showing concentric circles was placed over the dendritic image, the smallest circle was centered in the soma and the distance between each circle was equivalent to 10 μm apart. Total dendritic length was estimated by counting the total number of circle intersections and the density of dendrites was defined by counting the number of intersections on each circles. The confocal images of neurons were analyzed using Image J software (www.rcb.info.nih.gov/ij) which has plugged in Sholl analysis.

Stereotaxic surgery and infusions

Rats were anesthetized with xylazine (6 mg kg^{-1}, i.m., Lloyd laboratories, Shenandoar, IA) and ketamine (80 mg kg^{-1} i.m., Fort Dodge Animal Health, Overland Park, KS). Bilateral viral injections were performed with coordinates –3.5 mm (anterior/posterior), −0.5 mm (lateral), and −4.0 mm (dorsal/ventral) relative to the Bregma. A total of 3 μl of purified virus was delivered at a rate of 0.1μl min^{-1}. Needles were removed and the scalp incision

was closed with wound clips. After the behavioral testing was performed, animals were perfused with 4% paraformaldehyde. The brain was kept overnight in 4% paraformaldehyde and then transferred to 30% sucrose. 40 μm sections were cut using a microtome for visualization of GFP.

Learned Helplessness (LH) paradigm

The LH procedure was performed in custom built, 2-chambered shuttle boxes (Med Associates, Vermont) as previously described[45,46]. For active avoidance testing, animals were exposed to 30 escape trials using an FR1 schedule in which a single crossing terminated the footshock. Numbers of escape were automatically scored. Results are expressed as number of escape failures observed.

Forced swim test (FST)

FST was conducted as previously described[47]. On the test day, rats were placed for 10 min in a clear cylinder with water (24 ± 1°C, 45 cm depth). The sessions were recorded from the side and the immobility time was scored by a blind observer. Immobility was defined as floating or remaining motionless without leaning against the wall of the cylinder.

Locomotor Activity (LA)

To determine if there are general alterations in ambulation, locomotor activity was assessed. Rats were placed in clear plastic chambers fitted with automated activity meters (MED Associates, St. Albans, VT). Locomotor activity was recorded in 5-min bins for a total of 30 min.

Sucrose Preference test (SPT)

SPT was performed on day 21 after CUS. Animals were habituated to 1% sucrose solution (2%, Sigma, St. Louis, MO) for 3 d, followed by 6 h fluid deprivation on the test day. Rats were presented with two identical bottles, one containing 1% sucrose and the other water for 1 h and the consumption of each solution was measured. Sucrose preference was calculated as the percentage of sucrose consumed over total fluid consumption.

List of PCR primers used in this study for validation

mRNA expression

Gene	Forward (5'->3')	Reverse (3'->5')
CALM2	GGAATTAGTCCGAGTGGAGAG	TGCTCTTCAGTCAGTTGGTCA
SYN1	AGATTTTTGGGGGACTGGAC	TGACCACGAGCTCTACGATG
SYN3	CCAGATAGCTCCACCAGCTC	GGATCCTGGAGAGGAGAAGG
SYNGR3	AGCTGCTCCTCTCTCTGTGG	TAGGACAGGGCTGGTGTCTT
AMPH	CCAACCATGAAGAGGAAGGA	GAGGGTCCTGGATAGGCTTC
NRGN	GGCTCGGTAGGAGGAGTCTT	AGCACAGTCACATGCACACA
RAB3A	GGTGGTGTCATCAGAACGTG	GTCCAACGACTCGGACATCT
RAB4B	GGTCAGTGACGCGGAGTTAT	AGGGTCCAGGTCCTTCTTGT

mRNA expression

Gene	Forward (5'->3')	Reverse (3'->5')
TUBB2	AGCTCACCCAGCAGATGTTT	CATTTGCTCATCCACCTCCT
TUBB4	CTCGAGGCTTCTGACCTTTG	CCAGGGTCGGAGATGAAGTA
GATA1	CCAAGCTTCGTGGAACTCTC	AGGCGTTGCATAGGTAGTGG
PPIA	CTCGTGCCGTTTTGCAGAC	TGCAAACAGCTCAAAGGAGA
Calm2	AGCGAGTCGAGTGGTTGTCT	CCGTCGGCATCTACTTCATT
Syn1	CCAGCTCAACAAATCCCAGT	GGTGTCAGTCGGAGAAGAGG
Rab3a	GGTGGACGTGATCTGTGAGA	GAAGGGAAGTGTGGTTCAGC
Rab4b	ACTATTGGCGTGGAGTTTGG	CACAGAGGATGACCACGATG
Tubb4	GGGGACCTCAACCACCTAGT	ATCCTGGCATGAAGAAGTGG
Gata1	GATGGAATCCAGACGAGGAA	CTCTCCGCAATTCCCACTAC
Ppia	TTGCAGACGCCGCTGTCTCTT	TGGAACTTTGTCTGCAAACAGCTCG

GATA1 binding site

Gene	Forward (5'->3')	Reverse (3'->5')
Calm2	GGGAAGAAGATCCATGGAGAA	GGAGAATTCAGCCTGGAAAA
Syn1	ACAGCCTGCATCTCTCCATT	ATGTCTGCAAGGGTCCAAAG
Rab3a	CTGTCAAGGTCACAGCTTGG	GTAGCAGGACCACACACAGG
Rab4b	GGCCTGTGGGGTTAGAATTT	AAAAATCGGAGCAGAGACGA
Tubb4	CTGCCTCTTCGTCTCTAGCC	ACCGCTCAGGCTCACCTT

Supplementary Material

Refer to Web version on PubMed Central for supplementary material.

Acknowledgments

This work is supported by USPHS grants MH45481 (RSD), 2 P01 MH25642 (RSD), the Connecticut Mental Health Center (RSD), MH67996 (CAS), P20 RR17701 (CAS), and a National Research Foundation of Korea (NRF, No. 2011-0028317) (HS). We acknowledge the invaluable contributions made by the families consenting to donate brain tissue and be interviewed. We also thank the Cuyahoga County Coroner and staff, Cleveland, Ohio, for their willing assistance. The contributions of James Overholser, Ph.D., George Jurjus, M.D., Herbert Meltzer, M.D., Lisa Konick, Lisa Dieter, Nicole Herbst, Gouri Mahajan, Heather Kooiman and Justin Cobb in the psychiatric assessment and human tissue dissection and preparation are gratefully noted. We thank Dr. Tae Hoon Kim (Yale University) for his advice and suggestions regarding the binding motif analysis and chromatin immunoprecipitation. The pXM-GATA1 plasmid was kindly provided by Dr. Alan B. Cantor (Harvard) and pAAV-EGFP-pA vector was provided by Dr. Ralph J. Dileone (Yale). The GATA1 antibody was provided by Dr. Emery H. Bresnick (University of Wisconsin).

References

1. Rajkowska G, et al. Morphometric evidence for neuronal and glial prefrontal cell pathology in major depression. Biol. Psychiatry. 1999; 45:1085–1098. [PubMed: 10331101]
2. Drevets WC. Functional anatomical abnormalities in limbic and prefrontal cortical structures in major depression. Prog. Brain Res. 2000; 126:413–431. [PubMed: 11105660]
3. Lecrubier Y. The burden of depression and anxiety in general medicine. J. Clin. Psychiatry. 2001; 62(Suppl 8):4–9. [PubMed: 12108821]

4. Boyle LL, Porsteinsson AP, Cui X, King DA, Lyness JM. Depression predicts cognitive disorders in older primary care patients. J. Clin. Psychiatry. 2010; 71:74–79. [PubMed: 20129007]
5. Barabassy A, Beinhoff U, Riepe MW. Cognitive estimation in aged patients with major depressive disorder. Psychiatry Res. 2010; 176:26–29. [PubMed: 20064666]
6. Levens SM, Gotlib IH. Impaired selection of relevant positive information in depression. Depress. Anxiety. 2009; 26:403–410. [PubMed: 19347861]
7. Radley JJ, et al. Repeated stress induces dendritic spine loss in the rat medial prefrontal cortex. Cereb. Cortex. 2006; 16:313–320. [PubMed: 15901656]
8. Liu RJ, Aghajanian GK. Stress blunts serotonin- and hypocretin-evoked EPSCs in prefrontal cortex: role of corticosterone-mediated apical dendritic atrophy. Proc. Natl. Acad. Sci. U.S.A. 2008; 105:359–364. [PubMed: 18172209]
9. Bianchi M, Hagan JJ, Heidbreder CA. Neuronal plasticity, stress and depression: involvement of the cytoskeletal microtubular system? Curr. Drug Targets. CNS. Neurol. Disord. 2005; 4:597–611. [PubMed: 16266292]
10. Drevets WC, et al. Subgenual prefrontal cortex abnormalities in mood disorders. Nature. 1997; 386:824–827. [PubMed: 9126739]
11. Kang HJ, et al. Gene expression profiling in postmortem prefrontal cortex of major depressive disorder. J. Neurosci. 2007; 27:13329–13340. [PubMed: 18045927]
12. DeLorenzo RJ, Freedman SD. Calcium dependent neurotransmitter release and protein phosphorylation in synaptic vesicles. Biochem. Biophys. Res. Commun. 1978; 80:183–192. [PubMed: 23780]
13. DeCamilli P, Greengard P. Synapsin I: a synaptic vesicle-associated neuronal phosphoprotein. Biochem. Pharmacol. 1986; 35:4349–4357. [PubMed: 2878666]
14. Elferink LA, Scheller RH. Synaptic vesicle proteins and regulated exocytosis. Prog. Brain Res. 1995; 105:79–85. [PubMed: 7568899]
15. Wigge P, McMahon HT. The amphiphysin family of proteins and their role in endocytosis at the synapse. Trends Neurosci. 1998; 21:339–344. [PubMed: 9720601]
16. Belizaire R, et al. Characterization of synaptogyrin 3 as a new synaptic vesicle protein. J. Comp Neurol. 2004; 470:266–281. [PubMed: 14755516]
17. Zhong L, Cherry T, Bies CE, Florence MA, Gerges NZ. Neurogranin enhances synaptic strength through its interaction with calmodulin. EMBO J. 2009; 28:3027–3039. [PubMed: 19713936]
18. Brown TC, Correia SS, Petrok CN, Esteban JA. Functional compartmentalization of endosomal trafficking for the synaptic delivery of AMPA receptors during long-term potentiation. J. Neurosci. 2007; 27:13311–13315. [PubMed: 18045925]
19. Hoffman PN. Distinct roles of neurofilament and tubulin gene expression in axonal growth. Ciba Found. Symp. 1988; 138:192–204. [PubMed: 3058428]
20. Kim S, Webster MJ. Correlation analysis between genome-wide expression profiles and cytoarchitectural abnormalities in the prefrontal cortex of psychiatric disorders. Mol. Psychiatry. 2010; 15:326–336. [PubMed: 18762803]
21. Kim S, Webster MJ. Integrative genome-wide association analysis of cytoarchitectural abnormalities in the prefrontal cortex of psychiatric disorders. Mol. Psychiatry. 2011; 16:452–461. [PubMed: 20308991]
22. Tochigi M, et al. Gene expression profiling of major depression and suicide in the prefrontal cortex of postmortem brains. Neurosci. Res. 2008; 60:184–191. [PubMed: 18068248]
23. Sequeira A, et al. Global brain gene expression analysis links glutamatergic and GABAergic alterations to suicide and major depression. PLoS One. 2009; 4:e6585. [PubMed: 19668376]
24. Aston C, Jiang L, Sokolov BP. Transcriptional profiling reveals evidence for signaling and oligodendroglial abnormalities in the temporal cortex from patients with major depressive disorder. Mol. Psychiatry. 2005; 10:309–322. [PubMed: 15303102]
25. Tsang AP, et al. FOG, a multitype zinc finger protein, acts as a cofactor for transcription factor GATA-1 in erythroid and megakaryocytic differentiation. Cell. 1997; 90:109–119. [PubMed: 9230307]

26. Johnson KD, Kim SI, Bresnick EH. Differential sensitivities of transcription factor target genes underlie cell type-specific gene expression profiles. Proc. Natl. Acad. Sci. U.S.A. 2006; 103:15939–15944. [PubMed: 17043224]
27. Willner P. Validity, reliability and utility of the chronic mild stress model of depression: a 10-year review and evaluation. Psychopharmacology (Berl). 1997; 134:319–329. [PubMed: 9452163]
28. Baldelli P, Fassio A, Valtorta F, Benfenati F. Lack of synapsin I reduces the readily releasable pool of synaptic vesicles at central inhibitory synapses. J. Neurosci. 2007; 27:13520–13531. [PubMed: 18057210]
29. Geppert M, Goda Y, Stevens CF, Sudhof TC. The small GTP-binding protein Rab3A regulates a late step in synaptic vesicle fusion. Nature. 1997; 387:810–814. [PubMed: 9194562]
30. Matthews G. Calcium/calmodulin: a synaptic antidepressant? Neuron. 2001; 32:962–963. [PubMed: 11754827]
31. Pang ZP, Cao P, Xu W, Sudhof TC. Calmodulin controls synaptic strength via presynaptic activation of calmodulin kinase II. J. Neurosci. 2010; 30:4132–4142. [PubMed: 20237283]
32. Hoogenraad CC, et al. Neuron specific Rab4 effector GRASP-1 coordinates membrane specialization and maturation of recycling endosomes. PLoS. Biol. 2010; 8:e1000283. [PubMed: 20098723]
33. Gorwood P. [Severe depression: genes and the environment]. Encephale. 2009; 35(Suppl 7):S306–S309. [PubMed: 20141793]
34. Hammen C. Stress and depression. Annu. Rev. Clin. Psychol. 2005; 1:293–319. [PubMed: 17716090]
35. Viger RS, Guittot SM, Anttonen M, Wilson DB, Heikinheimo M. Role of the GATA family of transcription factors in endocrine development, function, and disease. Mol. Endocrinol. 2008; 22:781–798. [PubMed: 18174356]
36. Nardelli J, Thiesson D, Fujiwara Y, Tsai FY, Orkin SH. Expression and genetic interaction of transcription factors GATA-2 and GATA-3 during development of the mouse central nervous system. Dev. Biol. 1999; 210:305–321. [PubMed: 10357893]
37. Kala K, et al. Gata2 is a tissue-specific post-mitotic selector gene for midbrain GABAergic neurons. Development. 2009; 136:253–262. [PubMed: 19088086]
38. ElWakil A, Francius C, Wolff A, Pleau-Varet J, Nardelli J. The GATA2 transcription factor negatively regulates the proliferation of neuronal progenitors. Development. 2006; 133:2155–2165. [PubMed: 16672344]
39. Cole SW, et al. Computational identification of gene-social environment interaction at the human *IL6* locus. Proc. Natl. Acad. Sci. U.S.A. 2010; 107:5681–5686. [PubMed: 20176930]
40. Li N, et al. mTOR-dependent synapse formation underlies the rapid antidepressant effects of NMDA antagonists. Science. 2010; 329:959–964. [PubMed: 20724638]
41. Hajszan T, et al. Remodeling of hippocampal spine synapses in the rat learned helplessness model of depression. Biol. Psychiatry. 2009; 65:392–400. [PubMed: 19006787]
42. Hajszan T, et al. Effects of estradiol on learned helplessness and associated remodeling of hippocampal spine synapses in female rats. Biol. Psychiatry. 2010; 67:168–174. [PubMed: 19811775]
43. Noh JS, Gwag BJ. Attenuation of oxidative neuronal necrosis by a dopamine D1 agonist in mouse cortical cell cultures. Exp. Neurol. 1997; 146:604–608. [PubMed: 9270075]
44. SHOLL DA. Dendritic organization in the neurons of the visual and motor cortices of the cat. J. Anat. 1953; 87:387–406. [PubMed: 13117757]
45. Valentine G, Dow A, Banasr M, Pittman B, Duman R. Differential effects of chronic antidepressant treatment on shuttle box escape deficits induced by uncontrollable stress. Psychopharmacology (Berl). 2008; 200:585–596. [PubMed: 18604599]
46. Banasr M, et al. Chronic unpredictable stress decreases cell proliferation in the cerebral cortex of the adult rat. Biol. Psychiatry. 2007; 62:496–504. [PubMed: 17585885]
47. Pliakas AM, et al. Altered responsiveness to cocaine and increased immobility in the forced swim test associated with elevated cAMP response element-binding protein expression in nucleus accumbens. J. Neurosci. 2001; 21:7397–7403. [PubMed: 11549750]

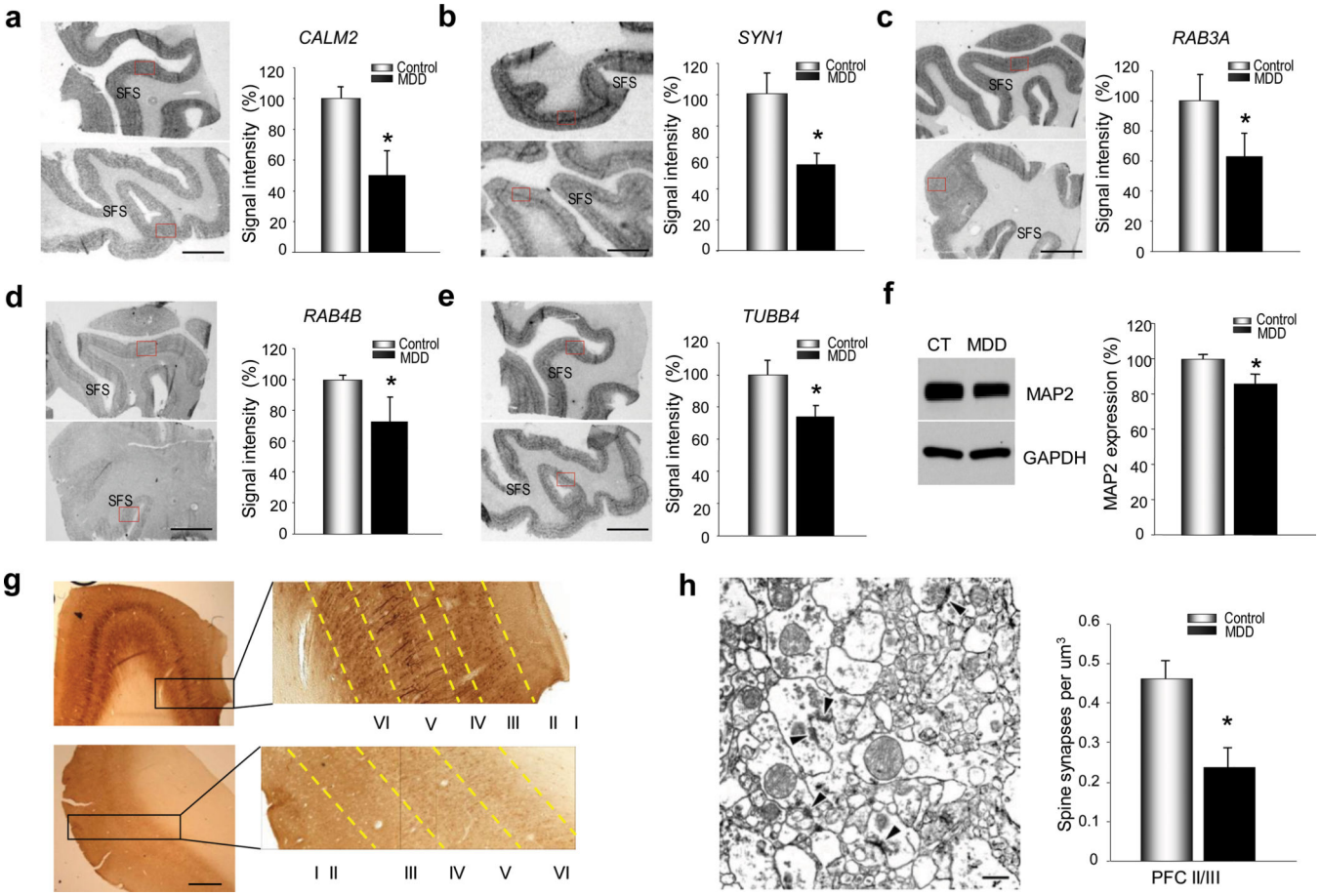

Figure 1.

Synaptic function-related genes, the number of spine synapses and MAP2 expression are decreased in dlPFC of MDD subjects. In situ hybridization analysis of five of the dysregulated genes that were confirmed by PCR analysis, including (**a**) calmodulin 2, (**b**) synapsin I, (**c**) Rab3A, (**d**) Rab4B, and (**e**) beta-tubulin 4. Representative images of the control (top) and MDD (bottom) autoradiographs (scale bar, 5 mm), and quantitative analysis (bar graphs) are shown. Results represent means ± S.E.M.s (n = 5). *P < 0.05 compared to control (unpaired t-test). (**f**) Levels of MAP2 were quantified by western blot analysis. Representative blot and quantitative results are shown. Results represent the mean ± S.E.M. (n = 4). *P < 0.05 compared to control (unpaired t-test). (**g**) Representative images of immunohistochemistry of MAP2 in dlPFC of control (upper) and MDD subjects (lower) (scale bar, 2 mm). (**h**) High power representative electron micrograph. Arrowheads point to examples of spine synapses (scale bar, 500 nm). Synapses were quantified in layer II/III of dlPFC (PFC II/III), and the results represent the mean ± SD (n = 5), *P < 0.05 compared to control (unpaired t-test).

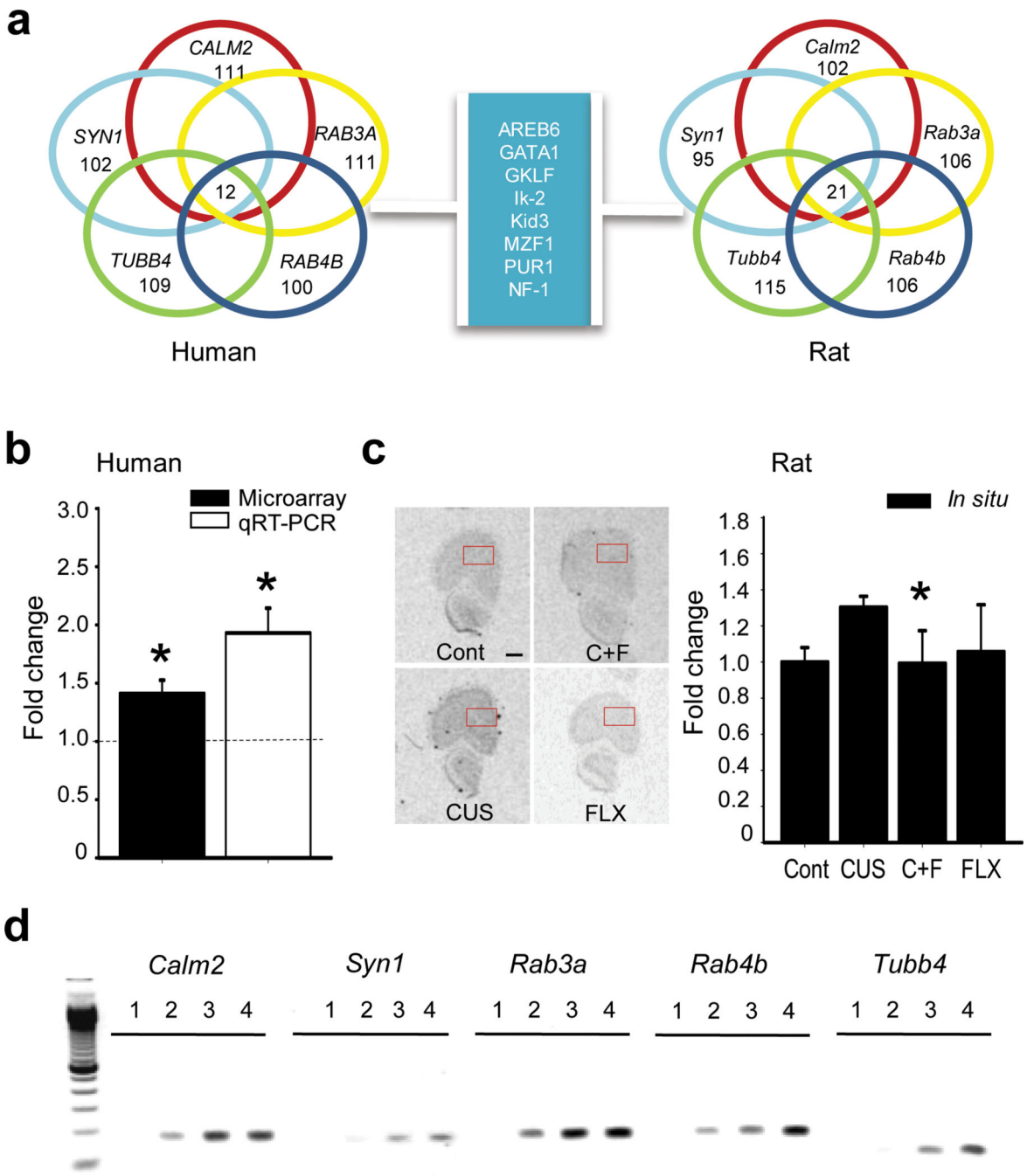

Figure 2.

Identification of a transcriptional repressor of synapse-related genes. (**a**) Summary of transcription factor binding motif analysis. To determine the common promoter elements in the 5 synapse related genes confirmed by qPCR, overlapping binding motifs were identified by Transfac analysis. Eight elements including GATA1 are present in the promoter regions of all the synapse related genes of both human and rat. (**b**) Expression of *GATA1* mRNA is increased in dlPFC of MDD subjects. Results from microarray and qPCR analysis of *GATA1* are shown, and represent the mean fold change relative to matched controls (n = 5

microarray pairs, and n = 10 pairs for PCR). *P <0.05 compared to control (unpaired t-test). (**c**) Influence of chronic unpredictable stress (CUS, 35 d) on the expression of *Gata1* in rat PFC was determined by in situ hybridization (representative image shown, scale bar, 1 mm). Increased expression of *Gata1* was reversed by fluoxetine administration for the last 21 d of CUS (C+F). Fluoxetine (FLX) alone did not influence *Gata1* expression. Results represent the mean ± S.E.M (n = 4); *P <0.05 compared to control (unpaired t-test). (**d**) Chromatin immunoprecipitation (ChIP) with GATA1 antiserum and PCR analysis of the putative GATA1 binding sites on the promoter regions of the synapse-related genes. Chromatin was immunoprecipitated using a GATA1 antibody and the presence of each gene was determined by PCR; lanes 1, no DNA; 2, horse serum ChIP (negative control); 3, GATA1 antibody ChIP; 4, total chromatin (positive control).

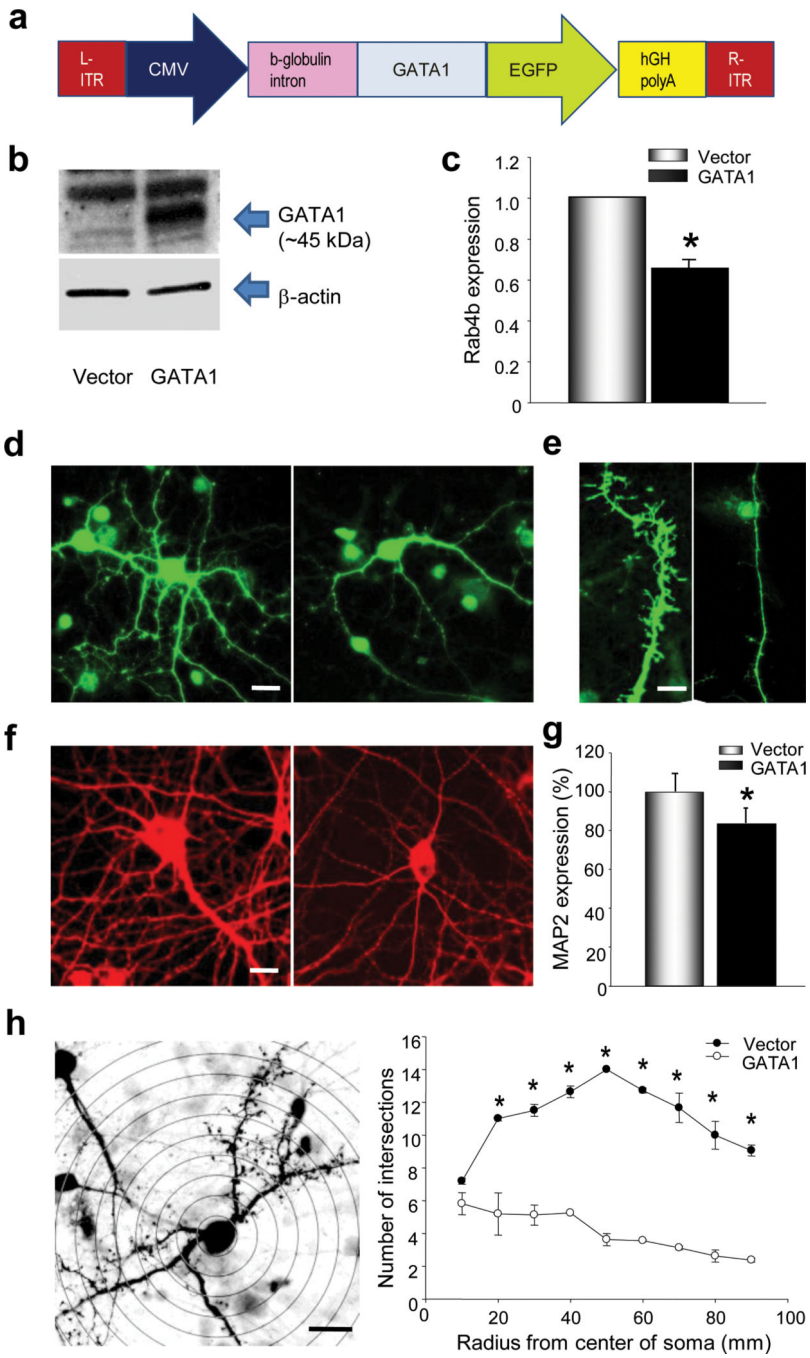

Figure 3.

GATA1 over-expression in cortical neurons decreases Rab4b expression and reduces dendrite branching. (**a**) rAAV-GATA1-EGFP vector construction. ITR, inverted terminal repeats; CMV, cytomegalovirus promoter; hGH-polyA, human growth hormone polyA signal (**b**) Levels of Gata1 protein, determined by western blot, are increased in response to rAAV-GATA1 infection; note that the size is shifted due to expression of conjugated GATA1-EGFP. (c) rAAV-GATA1 expression decreases levels of *Rab4b*determined by qRT-PCR. Cells were transfected at DIV5 and extracted at DIV19. Results of qPCR analysis

of *Rab4b* represent the mean ± S.E.M. (n = 4). *P <0.05 compared to vector alone (unpaired t-test). (**d**, **e**) Images of cortical neurons infected with control virus (left panels) or rAAV-GATA1-EGFP (right panels) and stained with antibodies to GFP (**d**, scale bar = 20 μm; **e**, scale bar = 10 μm). (**f**) Cells were infected with control virus (left panel) or rAAV-GATA1-EGFP (right panel) as described above but were stained for the dendritic marker MAP2 (scale bar = 20 μm), which was also examined by (**g**) western blot analysis (n = 3). *P <0.05 compared to vector alone (unpaired t-test). (**h**) Representative picture of Sholl analysis and quantitative results of the number of neuronal process intersections (scale bar = 20 μm). Results represent the mean ± S.E.M. (n = 7 for control vector, n = 4 for GATA1). *P <0.01 compared to vector alone (unpaired t-test).

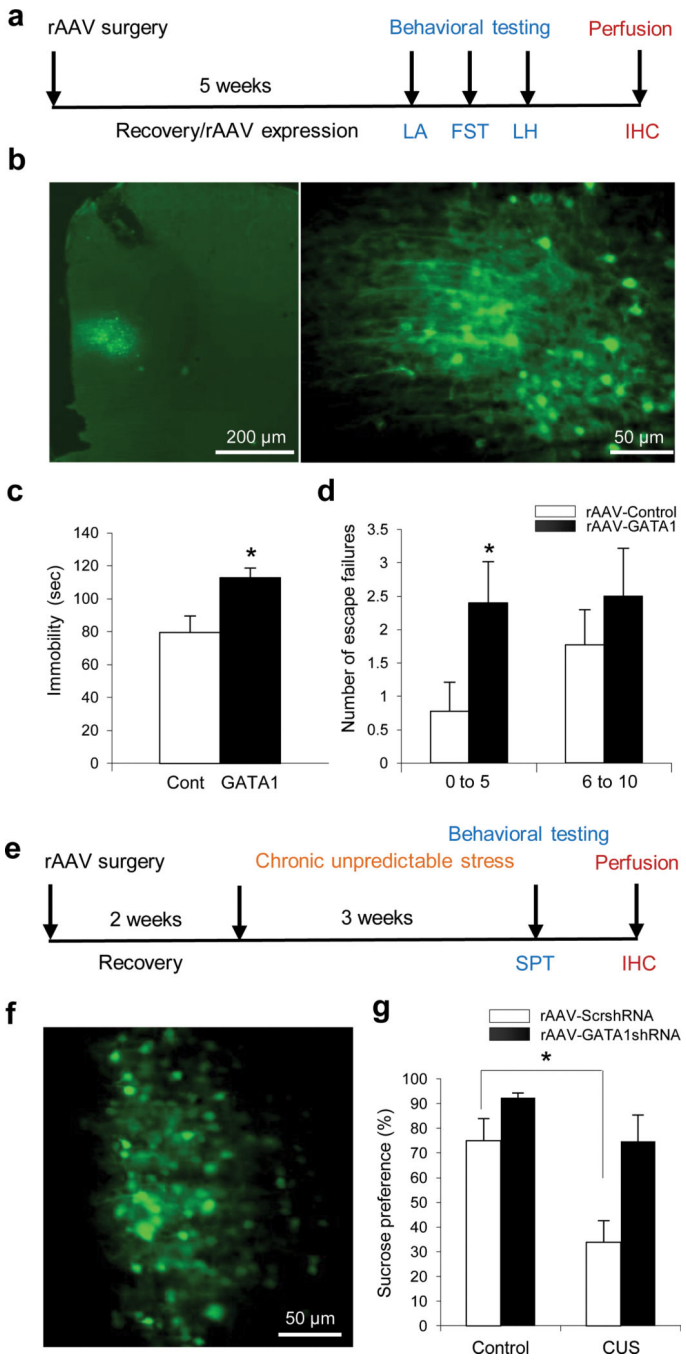

Figure 4.

Viral expression of GATA1 in rodent PFC causes depressive behavior. (**a**) Schematic diagram of the experimental schedule. (**b**) Representative low power (left panel) image of GFP immunohistochemistry (IHC) demonstrating the location of the viral infusion site in the medial PFC. The right panel shows the labeled neurons at higher magnification. (**c**,**d**) Influence of rAAV-control and rAAV-GATA1 on behavior in the forced swim test (FST, **c**) and learned helplessness (LH, **d**) paradigm. There was no effect on levels of locomotor activity (LA) (not shown). Results represent the mean ± S.E.M. (*n* = 9 for rAAV-control and

n = 10 for rAAV-GATA1). * $P < 0.05$ compared to rAAV-control (t-test). (**e**) Schematic diagram of *Gata1* shRNA knock down in the chronic unpredictable stress (CUS) paradigm. (**f**) Representative image of GFP immunohistochemistry demonstrating the location of viral infusion in the same region of the PFC as shown in b. (**g**) Influence of rAAV-ScrshRNA and rAAV-GATA1shRNA on sucrose preference in control and CUS exposed rats. Results represent the mean ± S.E.M. (Control: *n* = 6 for rAAV-ScrshRNA; *n* = 8 for rAAV-GATA1shRNA; CUS: *n* = 7 for rAAV-ScrshRNA; *n* = 8 for rAAV-GATA1shRNA). ** $P < 0.05$ compared to Control group (ANOVA and Fishers PLSD *post-hoc* analysis).

Nat Med. Author manuscript; available in PMC 2013 March 01.

Table 1

Gene	Genbank ID	Description	Fold Change (microarray)	P value (MAANOVA, FDR)	Fold Change (RT-PCR)	P value (t-test)
CALM2	BC008437	Calmodulin 2	0.55	0.004	0.81	0.03*
SYN1	NM_133499	Synapsin I	0.60	0.50	0.75	0.01*
SYN3	AF046873	Synapsin III	0.79	0.10	0.79	0.09
SYNGR3	NM_004209	Synaptogyrin 3	0.68	0.01	0.75	0.12
AMPH	U07616	Amphiphysin	0.77	0.10	0.89	0.62
NRGN	X99076	Neurogranin	0.80	0.10	0.84	0.09
RAB3A	BC011782	Ras-related GTP-binding protein 3A	0.75	0.40	0.80	0.00*
RAB4B	AF217985	Ras-related GTP-binding protein 4B	0.54	0.01	0.79	0.01*
TUBB2	NM_006088	Tubulin beta 2	0.60	0.01	0.79	0.06
TUBB4	BC000748	Tubulin beta 4	0.55	0.04	0.61	0.03*

Synaptic enriched genes were decreased in MDD. The results from the microarray were confirmed by real time PCR. All of the genes of interest were normalized to cyclophilin A. The results are presented as the mean ± SEM, $n = 15$ (microarray), $n = 8$ (RT-PCR), P values represent comparison to controls (unpaired t-test).